

Article

Impact of Inorganic Anions on the Photodegradation of Herbicide Residues in Water by UV/Persulfate-Based Advanced Oxidation

Gabriel Pérez-Lucas , Aitor Campillo and Simón Navarro * 

Department of Agricultural Chemistry, Geology and Pedology, School of Chemistry, University of Murcia, Campus Universitario de Espinardo, E-30100 Murcia, Spain; gpl2@um.es (G.P.-L.); aitor.campillo@um.es (A.C.)

* Correspondence: snavarro@um.es

Abstract: The removal of pesticides and other organic pollutants from water through advanced oxidation processes (AOPs) holds great promise. The main advantage of these technologies is that they remove, or at least reduce, pesticide levels by mineralization rather than transfer, as in conventional processes. This study first evaluated the effectiveness of UV/S₂O₈⁼ compared to heterogeneous photocatalysis using UV/TiO₂ processes on the degradation of two commonly used herbicides (terbuthylazine and isoproturon) in aqueous solutions using a laboratory photoreactor. In addition, the effect of the UV wavelength on the degradation efficiency of both herbicides was investigated. Although the degradation rate was greater under UV(254)/S₂O₈⁼ nm than under UV(365)/S₂O₈⁼ nm, complete degradation of the herbicides (0.2 mg L⁻¹) was achieved within 30 min under UV-366 nm using a Na₂S₂O₈ dose of 250 mg L⁻¹ in the absence of inorganic anions. To assess the impact of the water matrix, the individual and combined effects of sulfate (SO₄⁼), bicarbonate (HCO₃⁻), and chloride (Cl⁻) were evaluated. These can react with hydroxyl (HO•) and sulfate (SO₄•⁻) radicals generated during AOPs to form new radicals with a lower redox potential. The results showed negligible effects of SO₄⁼, while the combination of HCO₃⁻ and Cl⁻ seemed to be the key to the decrease in herbicide removal efficiency found when working with complex matrices. Finally, the main intermediates detected during the photodegradation process are identified, and the likely pathways involving dealkylation, dechlorination, and hydroxylation are proposed and discussed.

Keywords: matrix effect; herbicides; water treatment; persulfate; titanium dioxide; photooxidation



Citation: Pérez-Lucas, G.; Campillo, A.; Navarro, S. Impact of Inorganic Anions on the Photodegradation of Herbicide Residues in Water by UV/Persulfate-Based Advanced Oxidation. *Catalysts* **2024**, *14*, 376. <https://doi.org/10.3390/catal14060376>

Academic Editors: Yinsong Si, Xiufang Chen and Zhexin Zhu

Received: 14 May 2024

Revised: 6 June 2024

Accepted: 11 June 2024

Published: 13 June 2024



Copyright: © 2024 by the authors. Licensee MDPI, Basel, Switzerland. This article is an open access article distributed under the terms and conditions of the Creative Commons Attribution (CC BY) license (<https://creativecommons.org/licenses/by/4.0/>).

1. Introduction

Pesticides constitute an issue of considerable political interest in the fields of environment, agriculture, and human health under European legislation. The Directive on the Sustainable Use of Pesticides (2009/128/EC) [1] aims to reduce the risks and impacts of pesticide use on human health and the environment and to promote the use of integrated pest management and alternatives such as nonchemical approaches. In this context, water quality legislation is key to protecting public health and the environment in the European Union (EU). The Green Deal [2] and its associated strategies aim to reduce pesticide use and risks by 50% by 2030, with a focus on protecting ecosystems and enhancing biodiversity. For this purpose, the Water Framework Directive (WFD) 2000/60/EC [3] and its “daughter directives”, such as the Groundwater Directive (GWD) 2006/118/EC [4] and the Environmental Quality Standard Directive (EQSD) 2013/39/EU [5], help to protect European waters from pesticide and chemical pollution. In line with advances in science and technology over the past decades, on 26 October 2022, the EU Commission published its proposal to amend the WFD and EQSD [6]. These directives focus largely on so-called priority substances. In addition, the new Drinking Water Directive (DWD) 2020/2184 [7] sets quality objectives

for pesticides at the tap and includes a “*risk-based approach*”, provisions for the protection of raw water, and the consideration of pesticide metabolites.

However, since the adoption of the EU Urban Wastewater Treatment Directive (UWWTD) 91/271/EEC [8] in 1991, the quality of Europe’s rivers, lakes, and seas has improved dramatically. EU countries have used EU funding to build collection systems and wastewater treatment plants. However, there is still pollution that needs to be addressed and is not covered by current legislation. According to the European Environment Agency (EEA), a report based on data from Member States shows that only 38% of EU surface water bodies are in good chemical status, 46% are not in good chemical status, and 16% are in an unknown chemical status [9]. Another recent EEA technical report provides an overview of the occurrence of pesticides and their main metabolites (breakdown or reaction products) in surface water (lakes and rivers, 180 pesticides) and groundwater (159 pesticides), focusing on the European level (up to 39 European countries) from 2007 to 2017 [10]. This report shows exceedance rates of 5 to 15% for herbicides and 3 to 8% for insecticides in surface water, while in groundwater, the percentages were approximately 7% for herbicides and less than 1% for insecticides. Fungicides appeared to occur less frequently in both surface water and groundwater. To achieve maximum crop yields, herbicides are widely used. Agricultural activities, the cleaning of herbicide containers and equipment, and agricultural and herbicide manufacturing effluents are the main sources of herbicide water pollution. Two herbicides, isoproturon (ISP) and terbuthylazine (TBZ), are among the most frequently reported pesticides in surface water and groundwater in Europe. More recently, another study proposed a protocol for a systematic review and meta-analysis to determine the prevalence of pesticides in European water resources (watersheds, aquifers, rivers, the sea, and springs), wastewater (influent and effluent), and drinking water [11].

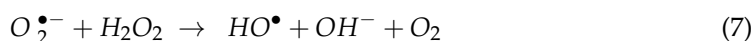
To address water pollution, the Commission has proposed an update to the Directive to enable a significant reduction in the discharge of pollutants into the EU’s lakes, rivers, and seas [12]. In this sense, for some of the most persistent pollutants, such as recalcitrant pesticides, the polluted water (from urban, agricultural, and industrial sources) treated by conventional wastewater treatment plants (WWTPs) is in some cases insufficient to achieve the legally required level of purity [13]. This issue is of particular concern in areas where low rainfall does not provide sufficient water resources to meet the needs of agriculture, which requires increased reuse of effluents coming from WWTPs. Water scarcity and the uneven geographical distribution of rainfall are concerns in arid and semiarid areas where water management strategies advocate the reuse of treated wastewater in agriculture due to climate change. The EU has also addressed this issue by revising the minimum requirements for water reuse in the context of integrated management under Regulation 2020/741/EU on minimum requirements for water reuse [14]. The aim of this regulation is to ensure the safety of recycled water for agricultural irrigation, promote circularity, support resilience to climate change, and contribute to the objectives of the WFD by addressing water scarcity and related pressures on water resources. Growing public concern about the presence of pesticides in both wastewater and drinking water is leading to the development of new regulations that will undoubtedly have an impact on the design and operation of wastewater treatment plants in the coming years.

As stated in the EQSD, the sources of pollution must be identified, and the emissions of pollutants must be treated at the source in the most economical, environmental, and sustainable way. Concerns have increased, as has the need to identify them and apply new and effective techniques for their reduction and elimination. Conventional water treatment processes and technologies reduce pollution significantly but not as much as the current regulations require. The refractory nature of some pesticides, which can be toxic to the microorganisms used, often renders biological treatments ineffective [15]. In addition, approaches based on adsorption, flocculation, and ion exchange are not fully effective because they do not destroy contaminants but rather transfer contaminants to a solid phase that requires subsequent treatment. Membrane technology has been used extensively in recent years to remove micropollutants from wastewater, but during long-term processes,

pollutants gradually accumulate in adsorbed materials until they reach saturation, after which they become inactive, and consequently, pollutant removal and membrane filtration efficiency decrease [16]; therefore, membrane technology is usually combined with other techniques, such as ozonation, activated carbon, or photooxidation [17].

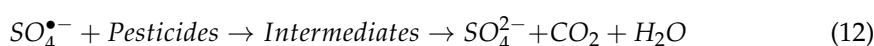
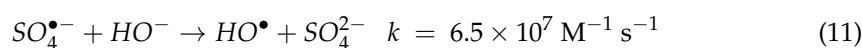
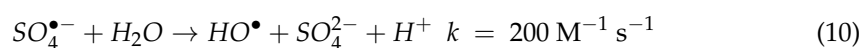
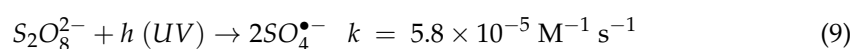
Advanced oxidation processes (AOPs) have been the most studied in recent years for the removal of pesticides and other micropollutants from wastewater [18–20]. Pesticides are oxidized by highly reactive oxygen species (ROS), mainly hydroxyl radicals ($\text{HO}^\bullet/\text{OH}^-$, $E^0 = 1.9\text{--}2.7$ V vs. NHE) and others such as superoxide anion ($\text{O}_2^{\bullet-}$) and hydroperoxy radical (HO_2^\bullet). The main advantage of these technologies is that they achieve the removal, or at least the reduction, of pesticide levels by mineralization rather than by transfer, as occurs in conventional processes [21]. These technologies are particularly useful in areas characterized by intensive agriculture and specific climatic patterns, where annual solar radiation is very high and water is scarce.

Among them, chemical reactions induced by a semiconductor photocatalyst that absorbs suitable radiation and remains unaffected during the process (heterogeneous photocatalysis) are of particular interest for water detoxification [22]. Semiconductors such as TiO_2 , ZnO , Fe_2O_3 , CdS , ZnS , and others can act as sensitizers for light-induced redox processes due to their electronic structure, which is characterized by a filled valence band (V_B) and an empty conduction band (C_B). The absorption of a photon with energy greater than the bandgap energy (E_g) leads to the formation of an electron (e^-)/hole (h^+) pair. In the absence of a suitable scavenger, the stored energy is dissipated by recombination within a few nanoseconds. If a suitable scavenger or surface defect is present to trap e^- or h^+ , recombination is prevented, and subsequent redox reactions can occur. The valence band h^+ is a strong oxidant ($E^0 = 1.0\text{--}3.5$ V vs. NHE) depending on the semiconductor and pH, while the conduction band e^- is a good reductant ($E^0 = 0.5$ to -1.5 V vs. NHE). Among the various semiconductor materials, TiO_2 ($E_g = 3.1$ eV) has been the most widely studied for environmental applications, mainly due to its nontoxicity, photostability, biological and chemical inertness, corrosion resistance, and chemical and thermal stability (over a wide pH range and at ambient pressure and temperature), among other properties. The photodegradation of pesticides in the presence of UV light and TiO_2 via redox reactions can be summarized according to the following mechanism [22]:

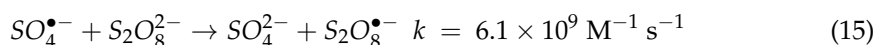
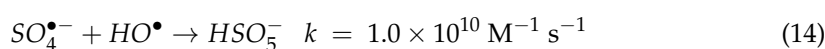
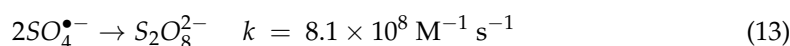


More recently, AOPs based on sulfate radical anions ($\text{SO}_4^{\bullet-}$) have received increasing attention as alternatives to conventional HO^\bullet -based AOPs [23–25]. $\text{SO}_4^{\bullet-}$ has a similar redox potential ($\text{SO}_4^{\bullet-}/\text{SO}_4^=$, $E^0 = 2.6\text{--}3.1$ V vs. NHE) to that of HO^\bullet , higher selectivity, and, in some cases, longer half-lives ($t_{1/2} = 30\text{--}40$ μs) than HO^\bullet ($t_{1/2} \leq 1$ μs), allowing more contact and transfer of mass between radical and organic compounds [26]. $\text{SO}_4^{\bullet-}$ is typically generated from peroxydisulfate ($\text{S}_2\text{O}_8^{2-}$, PDS), henceforth persulfate (PS) or peroxymonosulfate (HSO_5^- , PMS), which can be activated by energy (photochemical, sonochemical, and thermal), carbonaceous materials, electrochemical activation, alkaline conditions, transition metal ions, and various other oxidants such as ozone, hydrogen peroxide, and calcium peroxide [27,28]. PMS has a shorter bond length (1.460 Å) than PS

(1.497 Å), which explains its higher dissociation energy of the O-O bond (377 kJ mol⁻¹) compared to that of PS (92 kJ mol⁻¹) [23]. In most cases, UV/PS showed a better ability to oxidize organic pollutants than UV/PMS did. This can be attributed to the quantum yield of radical formation, as the quantum yield of PS₂₅₄ is approximately 1.8 M Einstein⁻¹, which is much greater than that of PMS₂₅₄ (0.5 M Einstein⁻¹) [23]. As a result, more energy is required for PMS to generate a radical during the homolytic cleavage of the peroxide bond [29]. In the thermal/photochemical decomposition pathway of PS, two moles of SO₄^{•-} are formed per mole of S₂O₈⁼ as a result of the cleavage of the peroxide bond (Equation (9)). SO₄^{•-} reacts with H₂O at all pH values to form HO[•] (Equation (10)), which is the primary reactive species under alkaline conditions (Equation (11)). At acidic (pH < 7) and alkaline (pH > 9) pH values, SO₄^{•-} and HO[•] are the dominant reactive species, respectively, while both radicals participate similarly in reactions at circumneutral pH [23,30]. Finally, SO₄^{•-} promotes the mineralization of pesticides to CO₂ and H₂O (Equation (12)) according to the following reactions:



However, both SO₄^{•-} and HO[•] undergo rapid and unwanted reactions (Equations (13)–(15)) where they are consumed, which may limit their effectiveness [31]:



In general, SO₄^{•-} is more susceptible to electron transfer reactions than is HO[•]. In contrast to SO₄^{•-}, HO[•] is more prone to hydrogen abstraction or addition [26,32]. Thus, SO₄^{•-}-based oxidation is an alternative oxidative treatment to AOPs based on HO[•] generation. SO₄^{•-} has several unique properties, such as being a very strong electron acceptor, which allows the degradation of persistent pesticides refractory to HO[•]. In addition, S₂O₈⁼, an environmentally friendly nontoxic oxidizer, avoids the problem of transport limitations because it is relatively stable and can be produced in high quantities.

Overall, the elimination of pesticides and other micropollutants by HO[•] and SO₄^{•-} based AOPs is largely influenced by the quality of the water matrix (dissolved constituents), which can be neutral, inhibitory, or promoting, depending on the process and the mechanism by which these water constituents react [23,33]. As with the experimental parameters, inorganic anions have an important influence on the performance of AOPs, although the influencing mechanisms of inorganic anions on their performance remain unclear. In general, inorganic anions can react with free radicals (usually called quenching effects), which affects the type and concentration of radicals, resulting in variations in the removal efficiency of the targeted organic pollutants. In addition to organic species, inorganic species such as Cl⁻, HCO₃⁻/CO₃²⁻, NO₃⁻/NO₂⁻, PO₄H³⁻, and/or SO₄²⁻, among others, can also act as inhibitors either by scavenging and generating radicals such as ClOH^{•-}, Cl[•], Cl₂^{•-}, CO₃^{•-}, HCO₃[•], Br[•], Br₂^{•-}, NO[•], and/or H₂PO₄[•], which have a lower E⁰ than HO[•] and SO₄^{•-} or by promoting the formation of ROS, as in the case of NO₃⁻, which is capable of generating HO[•] and NO₂[•] radical species that promote the photodegradation of pesticides, especially those for which indirect photolysis is the main reactive pathway. In summary, the effect of inorganic anions on the performance of AOPs is complex. It is related to the type of inorganic anion, the type of oxidant, the types of organic pollutants targeted, and the surface physicochemical properties of the catalysts in heterogeneous catalysis. To

accurately analyze the effect of inorganic anions on the performance of AOPs, it is necessary to understand their underlying influence mechanisms. Overall, the aim of this work was to evaluate the impact of inorganic ions on the removal of two herbicides (isoproturon and terbuthylazine) commonly found in wastewater using UV/persulfate-based advanced oxidation under laboratory conditions.

2. Results and Discussion

2.1. Photodegradation of Herbicides by UV, $\text{Na}_2\text{S}_2\text{O}_8$ and UV/ $\text{Na}_2\text{S}_2\text{O}_8$

The degradation efficiency of the herbicides was defined according to the following equation (Equation (16)):

$$R_e(\%) = \left(\frac{H_0 - H_t}{H_0} \right) \times 100 \quad (16)$$

where R_e is the removal efficiency, H_0 is the initial concentration of herbicide and H_t is the concentration of herbicide at time t .

UV radiation has been proposed as an effective method for removing herbicides from water [34]. Most herbicides are photoactive because their structure generally contains aromatic rings, heteroatoms, and other functional groups that make them susceptible to absorbing UV-Vis radiation (direct photolysis) or reacting with photosensitive species capable of inducing the photodegradation of herbicides in water (indirect photolysis). The results of herbicide degradation using UV (254/366 nm), UV (366 nm), PS alone, UV (254/366 nm)/PS, and UV (366 nm)/PS combined (trials 1–5) are shown in Figure 1.

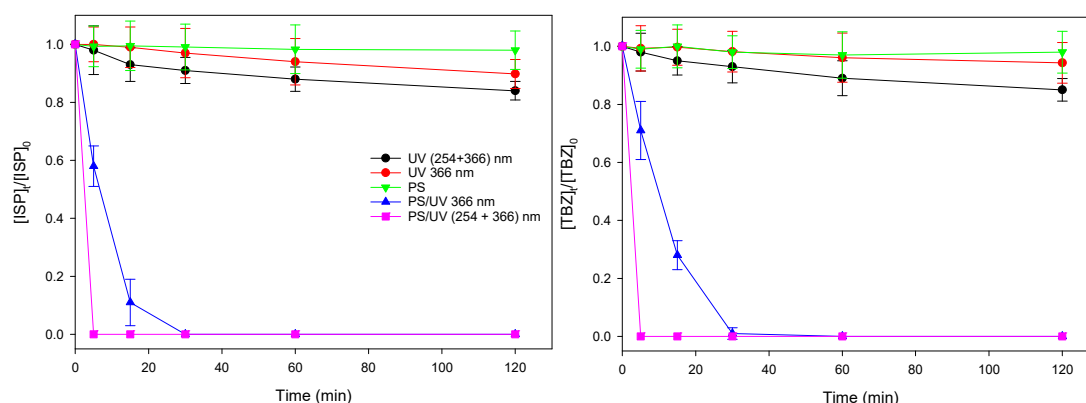


Figure 1. Evolution of herbicide residues over time in photolytic, PS, and UV/PS tests.

Minimal degradation (approximately 2% R_e) was observed for both herbicides when PS was used in the dark. When UV irradiation (254 or 366 nm) was used, the R_e of ISP increased to 16% (254 nm + 366 nm) and 10% (366 nm only), while TBZ removal was 15% (254 nm + 366 nm) and 7% (366 nm only) after a 120 min photoperiod. Some studies have shown that TBZ undergoes limited photodegradation and is considered photolytically and hydrolytically stable under environmentally relevant temperature and pH conditions [35]. However, photodegradation drastically increased in both cases when PS was activated with UV, either at a combined wavelength (254 + 366 nm) or at 366 nm only. After 5 min of irradiation (254 + 366 nm), the levels of both herbicides in the absence of inorganic anions were below LOD, whereas after 30 min of irradiation with 366 nm only, both herbicides practically disappeared. Similar results were obtained by Lin and Wu [36], who compared the effectiveness of PS activation at two wavelengths (254 nm and 365 nm) on the photodegradation of polyvinyl alcohol. PS activation by UV light might not be a promising method for industrial applications because of its high cost and complex equipment requirements. Although the activation of PS by UV/254 nm light improves the efficiency of the process, it is important to note that of the total radiant energy emitted by the Sun, only the part with a wavelength between 280–3000 nm, known as shortwave radiation, reaches the surface of our planet. This includes UVB (280–315 nm) and UVA

(315–400 nm) but not UVC (100–280 nm). Therefore, considering that the UVC fraction does not reach the Earth's surface, this fraction cannot be used in solar treatments for water purification because the spectrum of sunlight at the Earth's surface begins at approximately 300 nm. UV-366 nm/PS irradiation can therefore be considered an economical and effective process for the degradation of herbicides using natural sunlight. For this reason, the UVA fraction (366 nm) was used in subsequent tests because of the satisfactory results obtained.

2.2. Comparing UV/TiO₂ and UV/Na₂S₂O₈ Efficiencies

To compare the effectiveness of the two herbicides in degradation, UV/PS (test 5) and heterogeneous photocatalysis using UV/TiO₂ as a catalyst (test 6) were compared. Figure 2 shows the kinetic plots of both herbicides under these conditions. As seen, in both cases, a greater efficacy was observed for UV/PS than for UV/TiO₂, which is more notorious in the case of TBZ.

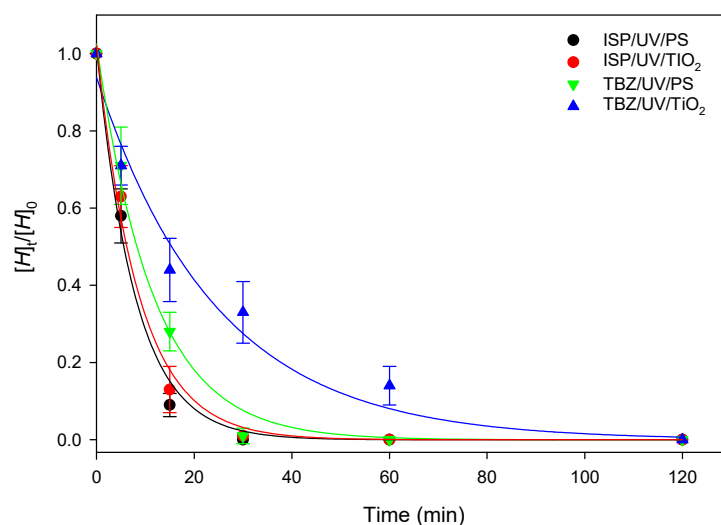


Figure 2. Degradation kinetics of herbicides in UV/PS and UV/TiO₂ systems.

According to the law of mass action, the photodegradation of herbicides can be modeled by assuming pseudo-first-order kinetics [37]. A kinetic study of the experimental results showed that the degradation process of both herbicides under UV basically conformed to the single first-order (SFO) kinetic model according to the following equations (Equations (17)–(19)):

$$-\frac{d[H]}{dt} = kt \quad (17)$$

$$[H]_t = [H]_0 e^{-kt} \quad (18)$$

$$\ln[H]_t = \ln[H]_0 - kt \quad (19)$$

where $[H]_t$ is the concentration of herbicide in solution at time t , $[H]_0$ is the initial herbicide concentration in solution, t is the time (min), and k is the apparent reaction rate constant (min^{-1}). The slope of $\ln(H_0/H_t)$ plotted against time gives the value of k . From the above equation, the time required for $X\%$ disappearance of herbicides (disappearance time) from the water can be calculated according to Equation (20):

$$DT_x = \ln \left(\frac{100}{100 - x} \right) / k \quad (20)$$

Consistent with the data obtained, the SFO model realistically fits the exponential decay curve with $R^2 \geq 0.97$ in all cases and a standard error of estimation ($S_{y/x}$) < 0.05 . The ratio between the apparent rate constants ($k_{\text{PS}}/k_{\text{TiO}_2}$) was > 1 in both cases, 1.1 for ISP and 3.3 for TBZ, indicating a higher reaction rate for both herbicides using UV/PS compared to

UV/TiO₂. For this reason, UV/PS was used to study the impact of inorganic anions on the photodegradation of the herbicides studied.

2.3. Effect of Inorganic Anion Content on Herbicide Photodegradation Using UV/Na₂S₂O₈

The effect of the composition of water on the photodegradation process is critical to assessing its suitability for real wastewater treatment, and its impact can be complex in some cases. In addition to dissolved organic matter, the unfavorable effects of some inorganic ions (mainly anions), such as Cl⁻, HCO₃⁻/CO₃²⁻, NO₃⁻/NO₂⁻, PO₄H³⁻, and/or SO₄²⁻, can be explained by the fact that they reduce the oxidizing power of the solution. The scavenging of HO[•] and SO₄^{•-} by various anions generates corresponding radicals such as ClOH^{•-}, Cl[•], Cl₂^{•-}, CO₃^{•-}, HCO₃[•], Br[•], Br₂^{•-}, NO[•], and/or H₂PO₄[•], which have a lower *E*⁰ than HO[•] and SO₄^{•-} or promote the formation of ROS, as in the case of NO₃⁻, which is capable of generating HO[•] and NO₂[•] radical species, which promote the photodegradation of pesticides, especially those for which indirect photolysis is the main reaction pathway [23,33,38]. Some anions and cations present in water are transparent to solar radiation, while nitrate (λ = 303 nm) and nitrite (λ = 355 nm) can absorb some of the radiation. Both absorb light and undergo homolysis to form HO[•] and reactive nitrogen species such as NO[•], NO₂[•], N₂O₃, and/or N₂O₄, leading to herbicide degradation, although HO[•] can be further scavenged by NO₂⁻ to form NO₂[•] [39]. However, the concentrations of NO₃⁻/NO₂ in real wastewater are usually low (<5 mg L⁻¹). For this reason, we assessed the influence of SO₄²⁻, Cl⁻, and HCO₃⁻, which are present at much higher concentrations.

As shown in Figure 3, the removal efficiency of the herbicides was not affected by the presence of sulfate at the concentration studied (250 mg L⁻¹). Even the presence of SO₄²⁻ in the solution (test 7) had a positive effect on the photodegradation of both herbicides, especially for ISP, because higher values of *k* were obtained according to the results shown in Table 1.

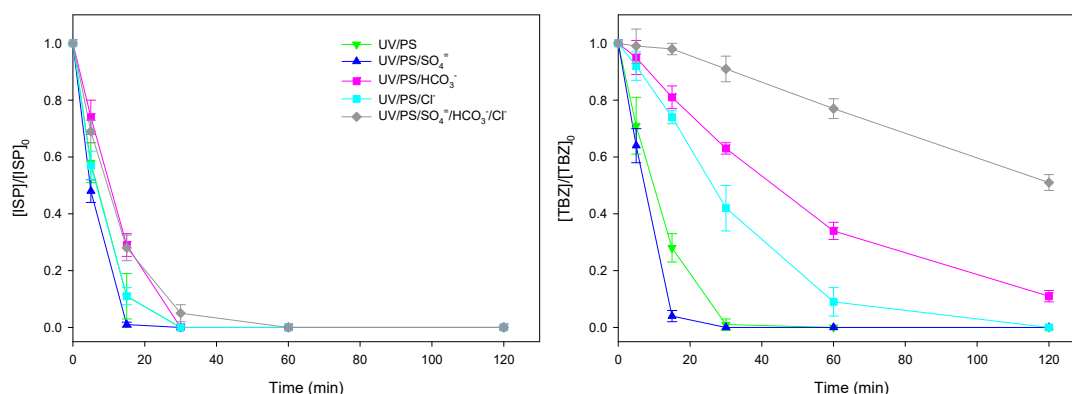


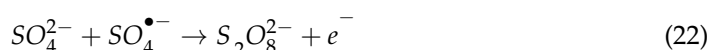
Figure 3. Anion-influenced UV/PS herbicide degradation.

Table 1. Kinetic parameters obtained following the SFO model for the photocatalytic degradation of herbicides in saline water.

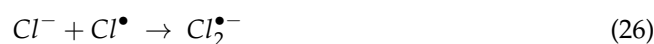
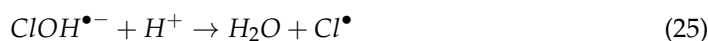
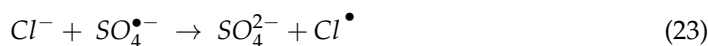
Anion	Terbutylazine (TBZ)				Isoproturon (ISP)			
	R	¹ k	² S _{y/x}	³ DT ₅₀	R	¹ k	² S _{y/x}	³ DT ₅₀
UV/PS	0.9952	0.1257	0.03	5.5	0.9953	0.1267	0.03	5.5
UV/PS/SO ₄ ²⁻	0.9755	0.1287	0.08	5.4	0.9917	0.1672	0.04	4.1
UV/PS/HCO ₃ ⁻	0.9963	0.0175	0.02	40	0.9875	0.0844	0.05	8.2
UV/PS/Cl ⁻	0.9829	0.0307	0.06	23	0.9961	0.1284	0.03	5.4
UV/PS/SO ₄ ²⁻ + HCO ₃ ⁻ + Cl ⁻	0.9755	0.0054	0.03	128	0.9979	0.0849	0.03	8.2

¹ (min⁻¹); ² Standard Error of Estimation; ³ (min).

$\text{SO}_4^=$ is not a strong scavenger of HO^\bullet , such as Cl^- , HCO_3^- , and CO_3^{2-} . In contrast, it has been shown to promote the oxidative degradation of the antibiotics chloramphenicol [40] and ciprofloxacin [41] or polyvinyl alcohol [36], as occurs in our case. According to Cabrera-Reina et al. [42], the removal efficiency of acetamiprid, carbamazepine, and caffeine was also unaffected by the sulfate concentration in the range of 0–550 mg L^{-1} . Therefore, the impact of $\text{SO}_4^=$ on activated PS processes, as summarized in Equations (21) and (22), is very low.



Chloride ions (Cl^-) are major inorganic anions in natural water. The adverse effect of Cl^- , especially at high concentrations, on the degradation of many organic micropollutants has been reported by some authors [23]. In the case of ISP, a minimal influence was observed when chloride ions (150 mg L^{-1}) were present in the solution because $k_{\text{PS}}/K_{\text{PS}/\text{Cl}}$ is 0.98 (Table 1). However, a significant influence was observed for TBZ, where the $k_{\text{PS}}/K_{\text{PS}/\text{Cl}}$ ratio was 4.1, as shown in Figure 3. The adverse effects of high Cl^- concentrations could favor the scavenging of HO^\bullet and $\text{SO}_4^{\bullet-}$ according to the following reactions (Equations (23)–(26)):



Compared to that of HO^\bullet -based AOPs, radical scavenging by Cl^- in $\text{SO}_4^{\bullet-}$ -based AOPs is a major challenge. The reaction between Cl^- and HO^\bullet gives $\text{ClOH}^{\bullet-}$ (Equation (24)), but this is a reversible reaction that mostly returns to HO^\bullet [43]. In contrast, $\text{SO}_4^{\bullet-}$ produces Cl^\bullet ($E^0 = 2.4$ V) by one-electron abstraction from Cl^- (Equation (23)), which is often reflected in lower efficiencies in organic pollutant removal as well as greater generation of reactive chlorine species such as $\text{Cl}_2^{\bullet-}$ ($E^0 = 2.1$ V), ClO_2^\bullet ($E^0 = 0.9$ V), (ClO^\bullet $E^0 = 1.4$ V), and $\text{ClOH}^{\bullet-}$ ($E^0 = 1.9$ V), all of which have lower E^0 than HO^\bullet and $\text{SO}_4^{\bullet-}$ [44].

An overall negative effect of HCO_3^- and CO_3^{2-} anions on $\text{SO}_4^{\bullet-}$ -based AOPs has traditionally been assumed [45]. The alkalinity of a water body is mainly influenced by CO_3^{2-} and HCO_3^- ions, which are generally present in natural waters at concentrations ranging from 50–250 mg L^{-1} . Both CO_3^{2-} and HCO_3^- are known to be radical scavengers in AOPs [23]. Among them, the radical scavenging ability of CO_3^{2-} is stronger than that of HCO_3^- due to its higher reaction rate constant with HO^\bullet ($3.9 \times 10^8 \text{ M}^{-1} \text{ s}^{-1}$ vs. $8.5 \times 10^6 \text{ M}^{-1} \text{ s}^{-1}$) [46].

However, depending on the chemical structure of the pesticide, the effect of $\text{HCO}_3^-/\text{CO}_3^{2-}$ on the degradation rate can be neutral, positive, or negative, which is very difficult to predict because complex mixtures of pollutants are always present in wastewater [47,48]. Although $\text{CO}_3^{\bullet-}$ has a lower redox potential than HO^\bullet , it could exhibit better removal performance in degrading organic micropollutants, which could be due to its high selectivity and longer survival time in solution [49].

When HCO_3^- was added, the initial pH of the aqueous solution changed to approximately 8.3 rather than 6.7 without the addition of any anions, and the alkaline conditions reduced the degradation efficiency of both herbicides, as discussed by some authors [50]. CO_2 , CO_3^{2-} , and HCO_3^- are present in aqueous media at $\text{pH} > 4$. CO_3^{2-} and HCO_3^- , which are responsible for water alkalinity, can compete with herbicides for HO^\bullet and $\text{SO}_4^{\bullet-}$ to generate other weaker radicals, such as $\text{CO}_3^{\bullet-}$ and/or HCO_3^\bullet . Above $\text{pH} = 10.3$, CO_3^{2-} is the prevalent species, but at pH values below 8.3, all CO_3^{2-} is converted to HCO_3^- [51]. As the pH decreases, the HCO_3^- concentration also decreases, and the dissolved CO_2

concentration increases (Figure 4). The relationship between $\text{CO}_3^{2-}/\text{HCO}_3^-$ and solution pH is represented as follows (Equation (27)):

$$\text{pH} = \text{p}K_a - \log \frac{[\text{HCO}_3^-]}{[\text{CO}_3^{2-}]} \quad \text{p}K_a = 10.3 \quad (27)$$

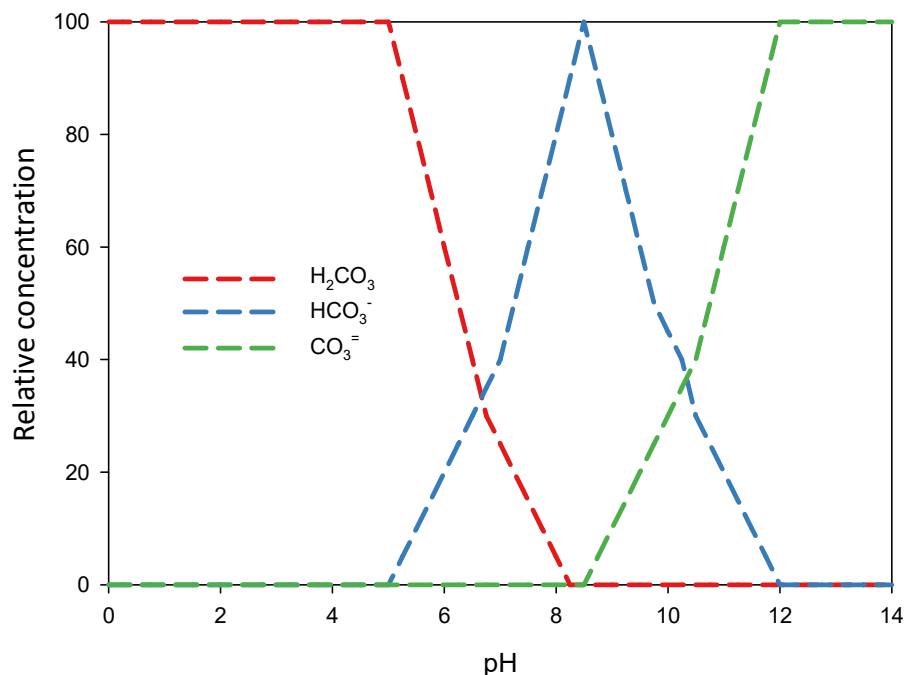
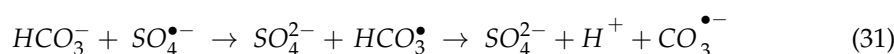
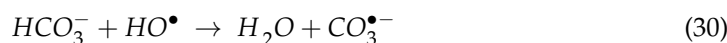
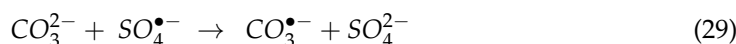


Figure 4. Speciation of carbonate species in water as a function of pH. Adapted from Manaham [51].

A high concentration (125 mg L^{-1}) of HCO_3^- strongly scavenges HO^\bullet and $\text{SO}_4^{\bullet-}$, generating electrophilic $\text{CO}_3^{\bullet-}$, a more selective and less reactive reaction radical with a lower electrode potential ($E^0 = 1.6 \text{ V}$) than HO^\bullet and $\text{SO}_4^{\bullet-}$ [52]. The detailed reaction mechanisms between $\text{CO}_3^{\bullet-}$ and micropollutants are still largely unclear. In previous studies, the single electron transfer pathway was determined to be the dominant pathway [46]. The nature of $\text{CO}_3^{\bullet-}$ makes it more selective toward electron-rich moieties such as $-\text{NH}_2$, $-\text{OH}$, and aromatic rings. HCO_3^\bullet has a lower reaction rate with organic pollutants than HO^\bullet does. Compared with HO^\bullet , $\text{SO}_4^{\bullet-}$ has a lower reaction rate with CO_3^{2-} ($6.1 \times 10^6 \text{ M}^{-1} \text{ s}^{-1}$) and a similar reaction rate to CO_3^{2-} ($9.1 \times 10^6 \text{ M}^{-1} \text{ s}^{-1}$) [53]. Nevertheless, the presence of $\text{CO}_3^{2-}/\text{HCO}_3^-$ can cause the transformation of HO^\bullet and $\text{SO}_4^{\bullet-}$, which can further affect the performance of AOPs. In radical-based treatment processes, $\text{CO}_3^{\bullet-}$ and HCO_3^\bullet can be formed by the oxidation of CO_3^{2-} and HCO_3^- with highly reactive radical species, such as HO^\bullet and $\text{SO}_4^{\bullet-}$ (Equations (28)–(31)) [54]:



In addition, carbonate precipitation can result in fouling of the membrane surface, which further affects the removal efficiency of micropollutants [55].

After studying the individual effects of $\text{SO}_4^{\bullet-}$, Cl^- , and HCO_3^- on the UV/PS process, their combined effect was then assessed (test 10). The R_e of both herbicides is presented in Figure 3. Cl^- (150 mg L^{-1}) and HCO_3^- (125 mg L^{-1}) generally had a negative effect

on the herbicide R_e , although the magnitude depended on the chemical structure of each herbicide. As shown in Table 1, the R values ranged from 0.976 to 0.996 for TBZ and from 0.988 to 0.998 for ISP, with standard errors of estimation less than 0.08 and 0.05, respectively, indicating a good fit. The time to 50% disappearance (DT_{50}) for ISP was slightly greater in the presence of anions (8.2 min) than in the corresponding experiment carried out in the absence of anions (5.5 min). However, a substantial effect was observed for TBZ, as the DT_{50} was approximately 23 times greater than that in the absence of anions, mainly due to the impact of HCO_3^- .

The initial pH of the aqueous solution of herbicides in the absence/presence of inorganic anions decreased in all cases during the photoperiod (Table 2). This decrease is less pronounced in the presence of HCO_3^- , the predominant species at $pH < 8.3$. Acidification may be caused by the formation of acidic products as a consequence of herbicide degradation and acidic photoproducts derived from $S_2O_8^{2-}$, such as HSO_4^- , with the release of H^+ (Equations (32) and (33)), as reported by Yang et al. [23]:

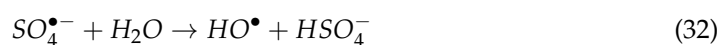


Table 2. Changes in pH during the different tests.

Time (min)	pH									
	Trial									
	1	2	3	4	5	6	7	8	9	10
0	6.70	6.74	5.09	5.11	5.04	5.33	4.69	8.29	5.20	8.39
5	6.53	6.56	4.97	5.02	5.00	5.15	4.60	8.20	4.79	8.36
15	6.42	6.41	4.81	4.88	4.84	4.93	4.46	8.23	4.46	8.39
30	6.29	6.33	4.58	4.60	4.64	4.84	4.29	8.24	4.20	8.40
60	6.15	6.19	4.23	4.34	4.38	4.75	4.01	8.21	3.93	8.35
120	6.07	6.14	3.86	3.88	3.95	4.61	3.77	8.07	3.66	8.25

In addition, the concentration of $SO_4^{\bullet-}$ increased significantly throughout the process (Equation (25)), as seen from the EC values shown in Table 3, due to the transformation of the initially added $S_2O_8^{2-}$ into $SO_4^{\bullet-}$. Various methods have been proposed to remove $SO_4^{\bullet-}$ from water in recent decades, such as adsorption on activated carbon, neutralization with calcium carbonate, biological treatment, reverse osmosis and dialysis, and ion exchange. The choice of wastewater treatment method is usually based on the type of wastewater, removal rate, waste concentration, and cost of treatment. Adsorption on an ion exchange resin is the most popular method for removing $SO_4^{\bullet-}$ from water and wastewater and shows good potential for industrial wastewater treatment [56].

Table 3. Evolution of electrical conductivity (EC) in the different tests.

Time (min)	EC ($\mu S\ cm^{-1}$)									
	Trial									
	1	2	3	4	5	6	7	8	9	10
0	<5	<5	242	238	242	<5	760	377	610	1200
5	<5	<5	248	245	249	7	764	380	620	1234
15	<5	<5	255	252	254	10	769	383	644	1253
30	<5	<5	261	263	260	12	773	386	662	1259
60	<5	<5	273	270	266	18	795	389	674	1262
120	<5	<5	285	287	280	23	825	395	700	1265

Figure 5 shows the evolution of the DOC during the different tests. It is important to monitor the process using this tool because only DOC values close to zero guarantee that recalcitrant pollutants or intermediates with greater persistence and toxicity than the initial ones do not persist. In the absence of any ions (UV/PS) and in the presence of SO_4^- (UV/PS/ SO_4^-), a high mineralization rate was observed because the remaining DOC after 120 min was less than 5%. However, in the presence of HCO_3^- (UV/PS/ HCO_3^-) and Cl^- (UV/PS/ Cl^-), the residual DOC concentrations after 120 min were 20% and 10%, respectively, while in the presence of all anions in the reaction solution (UV/PS/ $\text{SO}_4^- + \text{HCO}_3^- + \text{Cl}^-$), the residual DOC concentration at the end of the experiment significantly increased (37%). This residual DOC fraction may be due to the partial removal of herbicides in an aqueous solution and the formation of nondegradable organic intermediates during irradiation.

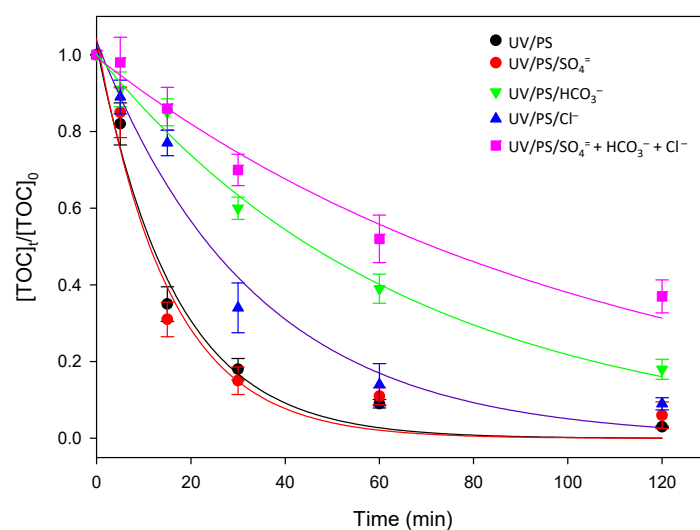


Figure 5. Evolution of DOC in the UV/PS system as a function of the anionic content.

2.4. Degradation Pathway of Herbicides with UV/ $\text{Na}_2\text{S}_2\text{O}_8$

To gain a better understanding of the reaction mechanisms involved in the photodegradation of both herbicides, the evolution of key intermediates during the irradiation experiment was also compared with authentic analytical standards using quantitative HPLC-MS² analysis. Figure 6 shows the proposed degradation pathways for both herbicides.

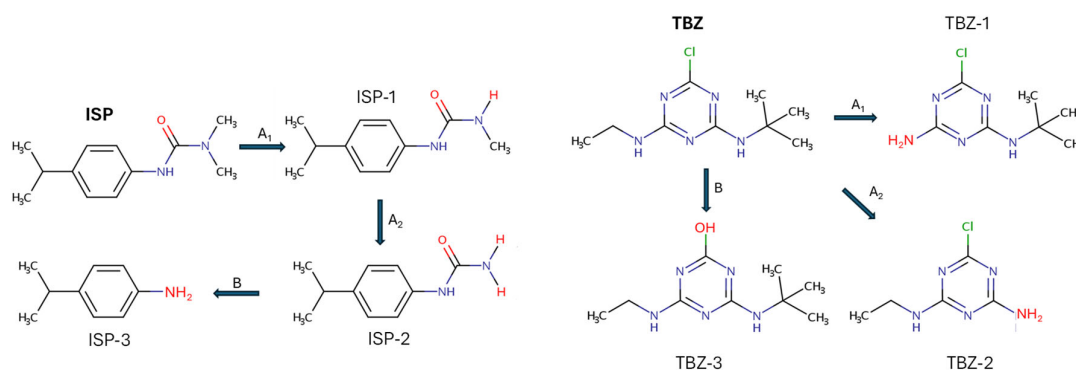


Figure 6. Proposed degradation pathways for ISP, including *N*-dealquylations (A1 and A2) and hydrolysis to aniline derivatives (B), and TBZ, involving dealkylations (A1 and A2), dechlorination, and subsequent hydroxylation (B).

The metabolic pathway involved in the degradation of ISP mainly involves two successive *N*-demethylations followed by hydrolysis to aniline-based metabolites, which

can then be further degraded. Photooxidation of TBZ leads to the dealkylation of the amine groups, dechlorination, and subsequent hydroxylation [57].

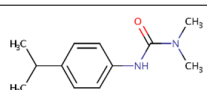
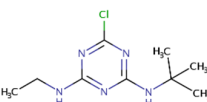
Three transformation products of ISP, isoproturon-monomethyl (ISP-1), isoproturon-desmethyl (ISP-2), and 4-isopropylaniline or cumidine (ISP-3), were identified during experiment 10, although their concentrations were below their LOQs ($<2 \mu\text{g L}^{-1}$) at the end of the photoperiod (120 min). The maximum concentration peak was found 30 min from the start, reaching levels between 4 and $8 \mu\text{g L}^{-1}$. These intermediates were also isolated by other authors in aqueous suspensions of TiO_2 and ZnO under UV light [58,59]. ISP is classified as moderately hazardous (class II) by the World Health Organization (WHO) and cataloged as an endocrine disruptor [60]. In the case of TBZ, photooxidation of the parent compound was accompanied by the presence of desethyl-terbuthylazine (TBZ-1), desisopropyl-atrazine (TBZ-2), and hydroxy-terbuthylazine (TBZ-3), whose residual levels after 120 min were in the range of 1.2, 0.6, and $0.5 \mu\text{g L}^{-1}$, respectively. TBZ, whose acceptable daily intake (ADI) is $0.004 \text{ mg kg}^{-1} \text{ bw day}^{-1}$, is classified by the WHO as slightly hazardous (class III), while metabolites are not listed. Fenoll et al. [61] found TBZ-1 and TBZ-3 intermediates using TiO_2 and ZnO as photocatalysts. The presence of these degradants confirms the behavior observed in the evolution of DOC, indicating that there is no total mineralization of the herbicides in the presence of anions. It should be remembered that for mineralization of the pollutant to occur, not only must it disappear, but all the organic carbon must also be converted into inorganic carbon in the form of CO_2 since the DOC value is independent of the oxidation state of the compounds present in the aqueous solution.

3. Materials and Methods

3.1. Herbicides, Solvents, and Reagents

Analytical standards of the herbicides isoproturon (ISP), terbuthylazine (TBZ), and their main metabolites were purchased from Dr. Ehrenstorfer GmbH (Augsburg, Germany), all with purities ranging from 95–99.5%. The main physicochemical characteristics of the herbicides studied are shown in Table 4. Titanium dioxide (70 anatase/30 rutile, 99.5%, BET $50 \text{ m}^2 \text{ g}^{-1}$, size $< 21 \text{ nm}$) Aeroxide™ P25 was obtained from Nippon Aerosil Co., Ltd. (Osaka, Japan). All HPLC-grade solvents (H_2O , CH_3CN , CH_3OH , and CH_2O_2) and reagents ($\text{Na}_2\text{S}_2\text{O}_8$, NaCl , Na_2SO_4 , and NaHCO_3) with purities $> 98.5\%$ were obtained from Scharlab (Barcelona, Spain).

Table 4. Main physicochemical properties of the herbicides studied.

Herbicide ¹	Structure	Formula	MW ²	$\text{S}_{\text{H}_2\text{O}}$ ³	$\log K_{\text{ow}}$ ⁴	H ⁵
Isoproturon ^{PU}		$\text{C}_{12}\text{H}_{18}\text{N}_2\text{O}$	206.3	70	2.5	1.5×10^{-5}
Terbuthylazine ^{TZ}		$\text{C}_9\text{H}_{16}\text{ClN}_5$	229.7	7	3.4	2.3×10^{-3}

¹ PU: Phenylurea; TZ: *s*-triazine; ² Molecular weight; ³ Water solubility (mg L^{-1}); ⁴ Partition coefficient n-octanol/water; ⁵ Henry Law constant ($\text{Pa m}^3 \text{ mol}^{-1}$).

3.2. Experimental Setup

The degradation of the herbicides was carried out by the $\text{UV}/\text{S}_2\text{O}_8^=$ or UV/TiO_2 process in a 2 L ($10 \text{ cm} \times 25 \text{ cm}$ long) Pyrex (jacketed borosilicate glass) batch cylindrical photoreactor (SBS, Barcelona, Spain) equipped with a magnetic stirrer, as previously described [62]. The study was carried out in batch circulation mode at a flow rate of 600 mL min^{-1} . The UV light source used was two Philips LIT 8 W (Amsterdam, The Netherlands) low-pressure mercury lamps with peak emissions at 254 and 366 nm. A typical irradiance of 10 mW cm^{-2} was measured using a Delta Ohm HD 2102.2 radiometer

(Caselle di Selvazzano, Italy). Nitrogen was continuously fed into the photoreactor at a flow rate of 0.5 L min^{-1} to ensure that oxygen did not interfere with the process. The system was thermostatically controlled by circulating water to maintain a constant temperature of $23 \pm 1 \text{ }^\circ\text{C}$. The photochemical reactor was filled with 2000 mL of Type II analytical grade water (pH 6.7, ORP 220 mV, conductivity $< 20 \text{ }\mu\text{S cm}^{-1}$, TOC $< 30 \text{ }\mu\text{g L}^{-1}$) and spiked with 0.2 mg L^{-1} of each herbicide. After the addition of $250 \text{ mg L}^{-1} \text{ Na}_2\text{S}_2\text{O}_8$ or $250 \text{ mg L}^{-1} \text{ TiO}_2$, the two UV lamps ($1 \times 254 \text{ nm} + 1 \times 366 \text{ nm}$ or $2 \times 366 \text{ nm}$) were switched on, and degradation was studied for 120 min. All experiments were replicated three times ($n = 3$). The initial pH of the water was 6.7. However, after the addition of $\text{Na}_2\text{S}_2\text{O}_8$, the pH decreased to approximately 5, while the addition of HCO_3^- increased the pH to 8.3. Table 5 summarizes the tests carried out.

Table 5. Summary of the trials carried out.

	Trials	pH	^a EC	^b $\text{SO}_4^{=}$	^b Cl^-	^b HCO_3^-
1	UV ($1 \times 254 \text{ nm} + 1 \times 366 \text{ nm}$)	6.7	<5	-	-	-
2	UV ($2 \times 366 \text{ nm}$)	6.7	<5	-	-	-
3	$\text{Na}_2\text{S}_2\text{O}_8$	5.1	240	-	-	-
4	$\text{Na}_2\text{S}_2\text{O}_8/\text{UV}$ (254/366 nm)	5.1	242	-	-	-
5	$\text{Na}_2\text{S}_2\text{O}_8/\text{UV}$ (366 nm)	5.0	246	-	-	-
6	TiO_2/UV (366 nm)	5.3	<5	-	-	-
7	$\text{Na}_2\text{S}_2\text{O}_8/\text{UV}$ (366 nm)	4.7	760	250	-	-
8	$\text{Na}_2\text{S}_2\text{O}_8/\text{UV}$ (366 nm)	8.3	377	-	-	125
9	$\text{Na}_2\text{S}_2\text{O}_8/\text{UV}$ (366 nm)	5.2	610	-	150	-
10	$\text{Na}_2\text{S}_2\text{O}_8/\text{UV}$ (366 nm)	8.4	1200	250	150	125

^a $\mu\text{S cm}^{-1}$; ^b mg L^{-1} .

3.3. Sample Preparation and Analytical Determinations

The sample (25 mL) was passed through an Oasis[®] HLB 60 μm (500 mg) extraction cartridge purchased from Waters (Milford, MA, USA) using a Visiprep[™] SPE vacuum manifold supplied by Supelco (Madrid, Spain) at a flow rate of approximately 3 mL min^{-1} . The extraction cartridge was previously conditioned with 3 mL of CH_3OH and equilibrated with 3 mL of acidified ultrapure water (pH = 3). After passing through the cartridge, the sample was washed with 5 mL of Milli-Q water ($18.2 \text{ M}\Omega\cdot\text{cm}$), the eluate was discarded, and the column was air-dried. The analytes were then eluted with 5 mL of CH_3OH and the extracts were evaporated to dryness. Finally, the residues were dissolved in 500 μL of CH_3CN and filtered through 0.22 μm polytetrafluoroethylene (PTFE) syringe filters prior to chromatographic analysis.

The determination of herbicide residues was carried out using an HPLC system consisting of a Waters e2695 separation module (Waters, Milford, CT, USA) equipped with a quaternary pump and an autosampler and coupled to a Waters 2998 photodiode array detector (PDA). The data were processed using Water Empower software (version 3). Separation was performed on a 100 mm \times 4.6 mm, 5 μm , Phenomenex Kinetex XB-C₁₈ analytical column (Madrid, Spain) with a mobile phase consisting of CH_3CN (solvent A) and an aqueous solution of HCOOH (0.1%) (solvent B) under gradient mode, with the temperature of the column oven set to $25 \text{ }^\circ\text{C}$. The following gradients were used: 30% of A for 1 min, linearly increased to 90% of A for 9 min, held for 1 min, and decreased to 30% of A for 2 min to allow equilibration before the next injection (5 min). The flow rate was maintained (0.5 mL min^{-1}), and the volume injected was 50 μL . The confirmation criteria were retention times and recovery wavelengths (190–400 nm). The detection wavelengths were 222 nm and 241 nm for TBZ and ISP, respectively. Standard solutions containing the herbicides were used to construct calibration curves ($0.1\text{--}1000 \text{ }\mu\text{g L}^{-1}$). The limits of detection (LODs) and limits of quantitation (LOQs) were obtained by dividing the signal-to-noise ratios 3 and 10 times, respectively, by the angular coefficients of the calibration curves. In addition, HPLC-MS² analysis of the intermediates generated during the UV/PS

process was performed on an Agilent (Santa Clara, CA, USA) 1200 HPLC system equipped with the same analytical column as previously described and coupled to an Agilent G6410A triple quadrupole (QqQ) mass spectrometer (MS) operating in electrospray ionization (ESI) positive ion mode. The most abundant fragment ion was selected for quantification, and the second was selected for identity confirmation. Data acquisition was performed using MassHunter software (V. 7.0).

The dissolved organic carbon (DOC) content was determined using a Multi N/C 3100 TOC Analyzer (Analytic Jena AG, Jena, Germany) after passing the samples through a nylon syringe filter (0.45 mm) prior to analysis to remove particulate OC from the sample. Both a GLP 21 pH meter and a GLP 31 conductivity meter (both from Crison Instruments, Barcelona, Spain) were used for pH and conductivity measurements, respectively. The statistical software SigmaPlot (Systat, Software Inc., San Jose, CA, USA) v.15 was used to fit the experimental data.

4. Conclusions

The need to increase the supply of water is linked to both the scarcity of the quantity available and the deterioration of its quality. Many families of chemical compounds, including pesticides, can have a negative impact on natural ecosystems and adversely affect water quality, thus posing a risk to human health. Many of them are carcinogenic, endocrine-disrupting, or even teratogenic and are highly persistent in the environment due to their complex structures and resistance to degradation. As a result of the current water scarcity, more emphasis should be placed on the 3Rs (recovery, recycle, and reuse) approach to wastewater treatment, both industrial and agricultural. For this reason, it is now essential to develop remediation techniques that favor the total elimination of all traces of pollutants in water, both of natural and anthropogenic origin, to promote its subsequent reuse, all with the aim of achieving the zero-pollution goal announced in the European Green Deal in relation to the Chemicals Sustainability Strategy.

Increasingly stringent environmental regulations regarding the presence of emerging pollutants in wastewater and natural systems have driven the need for treatment technologies that minimize environmental hazards at a reasonable cost. Conventional water treatment processes and technologies reduce water pollution significantly but not to the extent required by current legislation. The use of artificial UV light in photochemical processes may not be a promising method for environmental applications due to its high cost and the need for complex equipment. However, in the case of solar-powered applications, the process is not expensive because it uses sunlight radiation.

AOPs, which are usually applied after biological processes, have recently emerged as effective tertiary treatments for the removal of pesticides and other micropollutants, but the oxidation rates of individual compounds can be strongly influenced by the constituents of the water matrix. Overall, the removal of the studied herbicides (isoproturon and terbuthylazine) by HO^{\bullet} and $\text{SO}_4^{\bullet-}$ -based AOPs is largely influenced by the quality of the water matrix (dissolved constituents), which can be neutral, inhibitory, or promoting, depending on the process and the mechanism by which these water constituents react. In addition to organic species, inorganic species, mainly chloride and carbonate/bicarbonate ions, can also act as inhibitors, either by scavenging or by generating new radicals with a lower E^0 than HO^{\bullet} and $\text{SO}_4^{\bullet-}$. Herbicide photodegradation by UV/PS treatment is faster in pure water, largely due to the absence of organic and inorganic compounds that can absorb UV radiation and generate other ROS with lower oxidation potential.

Author Contributions: Conceptualization, S.N.; methodology, G.P.-L., A.C. and S.N.; investigation, G.P.-L., A.C. and S.N.; data curation, S.N.; writing—original draft preparation, G.P.-L. and S.N.; writing—review and editing, G.P.-L. and S.N.; supervision, S.N.; project administration, S.N.; funding acquisition, S.N. All authors have read and agreed to the published version of the manuscript.

Funding: This work was supported by the University of Murcia, Spain (Project 4711).

Data Availability Statement: The data will be made available upon request.

Conflicts of Interest: The authors declare no conflicts of interest.

References

1. EU. Directive 2009/128/EC of the European Parliament and of the Council of 21 October 2009 Establishing a Framework for Community action to achieve the sustainable use of pesticides. *Off. J. Eur. Union* **2009**, *L309*, 71–86. Available online: <https://eur-lex.europa.eu/legal-content/EN/TXT/PDF/?uri=CELEX:32009L0128> (accessed on 15 February 2024).
2. EC. Communication from the Commission to the European Parliament, the Council, the European Economic and Social Committee and the Committee of the Regions—The European Green Deal, COM/2019/640. 2019. Available online: <https://eur-lex.europa.eu/legal-content/EN/TXT/?uri=COM:2019:640:FIN> (accessed on 15 February 2024).
3. EU. Directive 2000/60/EC of the European Parliament and of the Council of 23 October 2000 establishing a framework for Community action in the field of water policy. *Off. J. Eur. Union* **2000**, *L327*, 1–73. Available online: <https://eur-lex.europa.eu/eli/dir/2000/60/oj> (accessed on 15 February 2024).
4. EU. Directive 2006/118/EC of the European Parliament and of the Council of 12 December 2006 on the protection of groundwater against pollution and deterioration. *Off. J. Eur. Union* **2006**, *L372*, 19–31. Available online: <https://eur-lex.europa.eu/legal-content/EN/TXT/PDF/?uri=CELEX:32006L0118> (accessed on 15 February 2024).
5. EU. Directive 2013/39/EU of the European Parliament and of the Council of 12 August 2013 amending Directives 2000/60/EC and 2008/105/EC as regards priority substances in the field of water policy. *Off. J. Eur. Union* **2013**, *L226*, 1–17. Available online: <https://eur-lex.europa.eu/LexUriServ/LexUriServ.do?uri=OJ:L:2013:226:0001:0017:en:PDF> (accessed on 15 February 2024).
6. EU. Proposal for a Directive of the European Parliament and of the Council amending Directive 2000/60/EC Establishing a Framework for Community Action in the Field of Water Policy, Directive 2006/118/EC on the Protection of Groundwater against Pollution and Deterioration and Directive 2008/105/EC on Environmental Quality Standards in the Field of Water Policy. COM/2022/540. 2022. Available online: <https://eur-lex.europa.eu/legal-content/EN/TXT/?uri=CELEX:52022PC0540> (accessed on 15 February 2024).
7. EU. EU Parliament Council Directive (EU) 2020/2184 of the European Parliament and of the Council of 16 December 2020 on the quality of water intended for human consumption (recast). *Off. J. Eur. Union* **2020**, *L435*, 1–62. Available online: <https://eur-lex.europa.eu/legal-content/EN/TXT/PDF/?uri=CELEX:32020L2184> (accessed on 15 February 2024).
8. EU. Council Directive of 21 May 1991 concerning urban wastewater treatment (91/271/EEC). *Off. J. Eur. Union* **1991**, *L135*, 40–91. Available online: <https://eur-lex.europa.eu/legal-content/EN/TXT/PDF/?uri=CELEX:31991L0271> (accessed on 15 February 2024).
9. EEA. *European Waters—Assessment of Status and Pressures 2018*; EEA Report No 7/2018; European Environment Agency: Copenhagen, Denmark, 2018; Available online: <https://www.eea.europa.eu/publications/state-of-water/> (accessed on 20 February 2024).
10. Mohaupt, V.; Völker, J.; Altenburger, R.; Birk, S.; Kirst, I.; Kühnel, D.; Küster, E.; Semeradova, S.; Šubelj, G.; Whalley, C. *Pesticides in European Rivers, Lakes and Groundwaters—Data Assessment*. European Topic Centre on Inland, Coastal and Marine Waters; Technical Report 1/2020; European Environment Agency: Magdeburg, Germany, 2020. [CrossRef]
11. Serrano-Valera, M.; Vela, N.; Piuvezam, G.; Mateo-Ramírez, F.; Santiago-Fernandes, I.D.; Martínez-Alcalá, I. Prevalence and concentration of pesticides in European waters: A protocol for systematic review and meta-analysis. *PLoS ONE* **2024**, *19*, e0282386. [CrossRef]
12. EC. Proposal for a Directive of the European Parliament and of the Council Concerning Urban Wastewater Treatment (Recast). SWD/2022/541. 2022. Available online: <https://eur-lex.europa.eu/legal-content/EN/TXT/PDF/?uri=CELEX:52022SC0541> (accessed on 15 February 2024).
13. Parida, V.K.; Saidulu, D.; Majumder, A.; Srivastava, A.; Gupta, B.; Gupta, A.K. Emerging contaminants in wastewater: A critical review on occurrence, existing legislations, risk assessment, and sustainable treatment alternatives. *J. Environ. Chem. Eng.* **2021**, *9*, e105966. [CrossRef]
14. EU. Regulation (EU) 2020/741 of the European Parliament and of the Council of 25 May 2020 on minimum requirements for water reuse. *Off. J. Eur. Union* **2020**, *L177*, 32–55. Available online: <https://eur-lex.europa.eu/legal-content/EN/TXT/PDF/?uri=CELEX:32020R0741> (accessed on 15 February 2024).
15. Alvarino, T.; Suarez, S.; Lema, J.; Omil, F. Understanding the sorption and biotransformation of organic micropollutants in innovative biological wastewater treatment technologies. *Sci. Total Environ.* **2018**, *615*, 297–306. [CrossRef]
16. Zhang, W.; Liang, W.; Zhang, Z.; Hao, T. Aerobic granular sludge (AGS) scouring to mitigate membrane fouling: Performance, hydrodynamic mechanism and contribution quantification model. *Water Res.* **2021**, *188*, e116518. [CrossRef] [PubMed]
17. Vasilachi, I.C.; Asimnicesei, D.M.; Fertu, D.I.; Gavrilescu, M. Occurrence and fate of emerging pollutants in water environment and options for their removal. *Water* **2021**, *13*, e181. [CrossRef]
18. Rout, P.R.; Zhang, T.C.; Bhunia, P.; Surampalli, R.Y. Treatment technologies for emerging contaminants in wastewater treatment plants: A review. *Sci. Total Environ.* **2021**, *753*, e141990. [CrossRef] [PubMed]
19. Saha, M.P. *Advanced Oxidation Processes for Effluent Treatment Plants*; Elsevier: Amsterdam, The Netherlands, 2021.
20. Soto-Verjel, J.; Maturana, A.Y.; Villamizar, S.E. Advanced catalytic oxidation coupled to biological systems to treat pesticide contaminated water: A review on technological trends and future challenges. *Water Sci. Technol.* **2022**, *85*, 1263–1294. [CrossRef] [PubMed]

21. Miklos, D.B.; Remy, C.; Jekel, M.; Linden, K.G.; Drewes, J.E.; Hübner, U. Evaluation of advanced oxidation processes for water and wastewater treatment—A critical review. *Water Res.* **2018**, *139*, 118–131. [[CrossRef](#)] [[PubMed](#)]
22. Augugliaro, V.; Palmisano, G.; Palmisano, L.; Soria, J. Heterogeneous photocatalysis and catalysis: An overview of their distinctive features. In *Heterogeneous Photocatalysis*; Marci, G., Palmisano, L., Eds.; Elsevier: Amsterdam, The Netherlands, 2019; pp. 1–24. [[CrossRef](#)]
23. Yang, Q.; Ma, Y.; Chen, F.; Yao, F.; Sun, J.; Wang, S.; Yi, K.; Hou, L.; Li, X.; Wang, D. Recent advances in photoactivated sulfate radical-advanced oxidation process (SR-AOP) for refractory organic pollutants removal in water. *Chem. Eng. J.* **2019**, *378*, e122149. [[CrossRef](#)]
24. Lee, J.; Von Gunten, U.; Kim, J.H. Persulfate-based advanced oxidation: Critical assessment of opportunities and roadblocks. *Environ. Sci. Technol.* **2020**, *54*, 3064–3081. [[CrossRef](#)] [[PubMed](#)]
25. Brillas, E. Activation of persulfate and peroxymonosulfate for the removal of herbicides from synthetic and real waters and wastewaters. *J. Environ. Chem. Eng.* **2023**, *11*, e110380. [[CrossRef](#)]
26. Olmez-Hanci, T.; Arslan-Alaton, I. Comparison of sulfate and hydroxyl radical based advanced oxidation of phenol. *Chem. Eng. J.* **2013**, *224*, 10–16. [[CrossRef](#)]
27. Oh, W.D.; Dong, Z.; Lim, T.T. Generation of sulfate radical through heterogeneous catalysis for organic contaminants removal: Current development, challenges and prospects. *App. Catal. B Environ.* **2016**, *194*, 169–201. [[CrossRef](#)]
28. Wang, J.; Wang, S. Activation of persulfate (PS) and peroxymonosulfate (PMS) and application for the degradation of emerging contaminants. *Chem. Eng. J.* **2018**, *334*, 1502–1517. [[CrossRef](#)]
29. Waclawek, S.; Lutze, H.V.; Grübel, K.; Padil, V.V.T.; Černík, M.; Dionysiou, D.D. Chemistry of persulfates in water and wastewater treatment: A review. *Chem. Eng. J.* **2017**, *330*, 44–62. [[CrossRef](#)]
30. Matzek, L.W.; Carter, K.E. Activated persulfate for organic chemical degradation: A review. *Chemosphere* **2016**, *151*, 178–188. [[CrossRef](#)] [[PubMed](#)]
31. Ren, W.; Huang, X.; Wang, L.; Liu, X.; Zhou, Z.; Wang, Y.; Lin, C.; He, M.; Ouyang, W. Degradation of simazine by heat-activated peroxydisulfate process: A coherent study on kinetics, radicals and models. *Chem. Eng. J.* **2021**, *426*, e131876. [[CrossRef](#)]
32. Serrano, K.G. Indirect Electrochemical Oxidation Using Hydroxyl Radical, Active Chlorine, and Peroxodisulfate. In *Electrochemical Water and Wastewater Treatment*; Martínez-Huitle, C.A., Rodrigo, M.A., Scialdone, O., Eds.; Elsevier: Amsterdam, The Netherlands, 2018. [[CrossRef](#)]
33. Ribeiro, A.R.L.; Moreira, N.F.F.; Li Puma, G.; Silva, A.M.T. Impact of water matrix on the removal of micropollutants by advanced oxidation technologies. *Chem. Eng. J.* **2019**, *363*, 155–173. [[CrossRef](#)]
34. Orellana-Garcia, F.; Alvarez, M.A.; Lopez-Ramon, V.; Rivera-Utrilla, J.; Sanchez-Polo, M.; Mota, A.J. Photodegradation of herbicides with different chemical natures in aqueous solution by ultraviolet radiation. Effects of operational variables and solution chemistry. *Chem. Eng. J.* **2014**, *255*, 307–315. [[CrossRef](#)]
35. ECHA. *Proposal for Harmonized Classification and Labeling*; CLH-227-637-9 Report for Terbutylazine; European Chemicals Agency: Merseyside, UK, 2014; Available online: <https://echa.europa.eu/substance-information/-/substanceinfo/100.025.125> (accessed on 20 March 2024).
36. Lin, C.C.; Wu, M.S. UV/S₂O₈²⁻ process for degrading polyvinyl alcohol in aqueous solutions. *Chem. Eng. Process.* **2014**, *85*, 209–215. [[CrossRef](#)]
37. Liu, B.; Zhao, X.; Terashima, C.; Fujishima, A.; Nakata, K. Thermodynamic and kinetics analysis of heterogeneous photocatalysis for semiconductor systems. *Phys. Chem. Chem. Phys.* **2014**, *16*, 8751–8760. [[CrossRef](#)]
38. Nafradi, M.; Alapi, T.; Bencsik, G.; Janaky, C. Impact of reaction parameters and water matrices on the removal of organic pollutants by TiO₂/LED and ZnO/LED heterogeneous photocatalysis using 365 and 398 nm radiation. *Nanomaterials* **2022**, *12*, e5. [[CrossRef](#)]
39. Mack, J.; Bolton, J.R. Photochemistry of nitrite and nitrate in aqueous solution: A review. *J. Photochem. Photobiol. A Chem.* **1999**, *128*, 1–13. [[CrossRef](#)]
40. Ghauch, A.; Baalbaki, A.; Amasha, M.; El Asmar, R.; Tantawi, O. Contribution of persulfate in UV-254 nm activated systems for complete degradation of chloramphenicol antibiotic in water. *Chem. Eng. J.* **2017**, *317*, 1012–1025. [[CrossRef](#)]
41. Lin, C.C.; Wu, M.S. Degradation of ciprofloxacin by UV/S₂O₈²⁻ process in a large photoreactor. *J. Photochem. Photobiol. A Chem.* **2014**, *285*, 1–6. [[CrossRef](#)]
42. Cabrera-Reina, A.; Aliste, M.; Polo-López, M.I.; Malato, S.; Oller, I. Individual and combined effect of ions species and organic matter on the removal of microcontaminants by Fe³⁺-EDDS/solar-light activated persulfate. *Water Res.* **2023**, *230*, e119566. [[CrossRef](#)]
43. Buxton, G.V.; Greenstock, C.L.; Helman, W.P.; Ross, A.B. Critical review of rate constants for reactions of hydrated electrons, hydrogen atoms and hydroxyl radicals in aqueous solution. *J. Phys. Chem. Ref. Data* **1988**, *17*, 513–886. [[CrossRef](#)]
44. Armstrong, D.A.; Huie, R.E.; Koppenol, W.H.; Lymar, S.V.; Merényi, G.; Neta, P.; Ruscic, B.; Stanbury, D.M.; Steenken, S.; Wardman, P. Standard electrode potentials involving radicals in aqueous solution: Inorganic radicals (IUPAC Technical Report). *Pure Appl. Chem.* **2015**, *87*, 1139–1150. [[CrossRef](#)]
45. Bennedsen, L.R.; Muff, J.; Søgaard, E.G. Influence of chloride and carbonates on the reactivity of activated persulfate. *Chemosphere* **2012**, *86*, 1092–1097. [[CrossRef](#)]

46. Canonica, S.; Kohn, T.; Mac, M.; Real, F.J.; Wirz, J.; von Gunten, U. Photosensitizer method to determine rate constants for the reaction of carbonate radical with organic compounds. *Environ. Sci. Technol.* **2005**, *39*, 9182–9188. [[CrossRef](#)]
47. Acero, J.L.; Benítez, F.J.; Real, F.J.; Rodríguez, E. Degradation of selected emerging contaminants by UV-activated persulfate: Kinetics and influence of matrix constituents. *Sep. Purif. Technol.* **2018**, *201*, 41–50. [[CrossRef](#)]
48. Lebig-Elhadi, H.; Frontistis, Z.; Ait-Amar, H.; Madjene, F.; Mantzavinos, D. Degradation of pesticide thiamethoxam by heat-activated and ultrasound-activated persulfate: Effect of key operating parameters and the water matrix. *Process Saf. Environ. Prot.* **2020**, *134*, 197–207. [[CrossRef](#)]
49. Sbardella, L.; Gala, I.V.; Comas, J.; Layret, R.R.; Gernjak, W. The impact of wastewater matrix on the degradation of pharmaceutically active compounds by oxidation processes including ultraviolet radiation and sulfate radicals. *J. Hazard. Mater.* **2019**, *380*, e120869. [[CrossRef](#)]
50. Lin, C.C.; Lee, L.T.; Hsu, L.J. Performance of UV/S₂O₈²⁻ process in degrading polyvinyl alcohol in aqueous solutions. *J. Photochem. Photobiol. A Chem.* **2013**, *252*, 1–7. [[CrossRef](#)]
51. Manaham, S.E. *Environmental Chemistry*, 9th ed.; CRC Press: Boca Raton, FL, USA, 2010.
52. Zuo, Z.; Cai, Z.; Katsumura, Y.; Chitose, N.; Muroya, Y. Reinvestigation of the acid–base equilibrium of the (bi) carbonate radical and pH dependence of its reactivity with inorganic reactants. *Radiat. Phys. Chem.* **1999**, *55*, 15–23. [[CrossRef](#)]
53. Ma, J.; Yang, Y.; Jiang, X.; Xie, Z.; Li, X.; Chen, C.; Chen, H. Impacts of inorganic anions and natural organic matter on thermally activated persulfate oxidation of BTEX in water. *Chemosphere* **2018**, *190*, 296–306. [[CrossRef](#)]
54. Xiao, R.; Meng, Y.; Fu, Y.; Waclawek, S.; Wei, Z.; Spinney, R.; Dionysiou, D.; Hu, W.P. The overlooked carbonate radical in micropollutant degradation: An insight into hydration interaction. *Chem. Eng. J.* **2023**, *474*, e145245. [[CrossRef](#)]
55. Mikhaylin, S.; Bazinet, L. Fouling on ion-exchange membranes: Classification, characterization and strategies of prevention and control. *Adv. Colloid Interface Sci.* **2016**, *229*, 34–56. [[CrossRef](#)]
56. Haghsheno, R.; Mohebbi, A.; Hashemipour, H.; Sarraf, A. Study of kinetic and fixed bed operation of removal of sulfate anions from an industrial wastewater by an anion exchange resin. *J. Hazard. Mater.* **2009**, *166*, 961–966. [[CrossRef](#)]
57. Roberts, T.; Hutson, D. Metabolic Pathways of Agrochemicals. In *Part One: Herbicides and Plant Growth Regulators*; The Royal Society of Chemistry: Cambridge, UK, 1998.
58. Haque, M.M.; Muneer, M. Heterogeneous photocatalyzed degradation of an herbicide derivative, isoproturon in aqueous suspension of titanium dioxide. *J. Environ. Manag.* **2003**, *69*, 169–176. [[CrossRef](#)]
59. Fenoll, J.; Sabater, P.; Navarro, G.; Pérez-Lucas, G.; Navarro, S. Photocatalytic transformation of sixteen substituted phenylurea herbicides in aqueous semiconductor suspensions: Intermediates and degradation pathways. *J. Hazard. Mater.* **2013**, *244*, 370–379. [[CrossRef](#)]
60. Lewis, K.A.; Tzilivakis, J.; Warner, D.J.; Green, A. An international database for pesticide risk assessments and management. *Hum. Ecol. Risk Assess.* **2016**, *22*, 1050–1064. [[CrossRef](#)]
61. Fenoll, J.; Hellin, P.; Martínez, C.M.; Flores, P.; Navarro, S. Semiconductor-sensitized photodegradation of s-triazine and chloroacetanilide herbicides in leaching water using TiO₂ and ZnO as catalyst under natural sunlight. *J. Photochem. Photobiol. A Chem.* **2012**, *238*, 81–87. [[CrossRef](#)]
62. Vela, N.; Fenoll, J.; Garrido, I.; Navarro, G.; Gambín, M.; Navarro, S. Photocatalytic mitigation of triazinone herbicide residues using titanium dioxide in slurry photoreactor. *Catal. Today* **2015**, *252*, 70–77. [[CrossRef](#)]

Disclaimer/Publisher’s Note: The statements, opinions and data contained in all publications are solely those of the individual author(s) and contributor(s) and not of MDPI and/or the editor(s). MDPI and/or the editor(s) disclaim responsibility for any injury to people or property resulting from any ideas, methods, instructions or products referred to in the content.